# 3-(Piperidin-4-ylmethoxy)pyridine Containing Compounds Are Potent Inhibitors of Lysine Specific Demethylase 1

Fangrui Wu,[†,§] Chao Zhou,[†,§] Yuan Yao,[†] Liping Wei,[†] Zizhen Feng,[†] Lisheng Deng,[†] and Yongcheng Song*[,†,‡]

[†]Department of Pharmacology, and [‡]Dan L. Duncan Cancer Center, Baylor College of Medicine, 1 Baylor Plaza, Houston, Texas 77030, United States

S Supporting Information

ABSTRACT: Methylation of histone lysine residues plays important roles in gene expression regulation as well as cancer initiation. Lysine specific demethylase 1 (LSD1) is responsible for maintaining balanced methylation levels at histone H3 lysine 4 (H3K4). LSD1 is a drug target for certain cancers, due to important functions of methylated H3K4 or LSD1 overexpression. We report the design, synthesis, and structure−activity relationships of 3-(piperidin-4-ylmethoxy)-pyridine containing compounds as potent LSD1 inhibitors with K_i values as low as 29 nM. These compounds exhibited high selectivity (>160×) against related monoamine oxidase A and B. Enzyme kinetics and docking studies suggested they are competitive inhibitors against a dimethylated H3K4 substrate and provided a possible binding mode. The potent LSD1 inhibitors can increase cellular H3K4 methylation and strongly inhibit proliferation of several leukemia and solid tumor cells with EC_{50} values as low as 280 nM, while they had negligible effects on normal cells.

K_i as low as 29 nM — Cancer cell EC_{50}: 0.28 − 5 μM
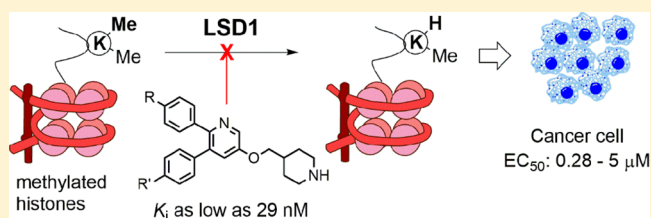
INTRODUCTION

Post-translational modifications of the ε-amino group of histone lysine residues, such as acetylation and methylation, play important roles in gene expression regulation in normal physiology as well as diseases.[1−4] Small molecule modulators of histone modifying enzymes are therefore chemical probes for biological studies and potentially useful therapeutics for such diseases.[5−7] Histone H3 lysine 4 (H3K4) methylation, including mono-, di-, and trimethylation (H3K4me1, -2, and -3) has been found to be generally a biomarker for active gene transcription.[8,9] Mixed lineage leukemia (MLL), a large, multidomain protein containing ∼4000 amino acids, can methylate H3K4, with its C-terminal SET domain being catalytically active.[9−11] In addition, cellular H3K4 methylation levels are tightly regulated because of their important functions. Lysine specific demethylase 1 (LSD1, also known as KDM1a), has been found to be a member of an MLL transcription complex. LSD1 catalyzes an oxidative demethylation reaction from H3K4me1 and -2 (but not H3K4me3) and thus counteracts the enzyme function of MLL.[12,13] Both MLL and LSD1 are essential for hematopoiesis, showing a balanced cellular H3K4 methylation is crucial for normal hematopoiesis.[11,14] In addition, H3K9[15] and other proteins such as DNMT1[16] were reported as a substrate of LSD1.

Dysregulated histone lysine methylations may lead to a disease, such as cancer.[2] For example, ∼75% acute leukemia in infants and 10% of that in adults contain an MLL gene translocation and this subtype of leukemia shows a poor prognosis.[17−19] All MLL translocations identified to date produce an onco-MLL fusion protein without the C-terminal

SET domain, which cannot methylate H3K4.[11] Rather, the fusion partners can recruit DOT1L, a histone H3 lysine 79 (H3K79) methyltransferase, which causes aberrant H3K79 methylation at MLL target gene loci and overexpression of these genes, eventually leading to the initiation of the leukemia.[20−22] Pharmacological inhibition of DOT1L has been found to block proliferation of MLL-rearranged leukemia cells, showing effectiveness of the targeted epigenetic therapy.[23,24]

LSD1 is a flavin adenine dinucleotide (FAD) dependent oxidase, related to monoamine oxidase A and B (MAO-A and -B).[13] Figure 1A schematically shows the mechanism of catalysis of LSD1. Upon binding to LSD1, the methyl group of a methylated histone lysine residue (e.g., H3K4me2) is oxidized by the cofactor FAD, followed by hydrolysis to give formaldehyde and demethylated lysine. $FADH_2$, the reduced form of FAD, is oxidized by O_2 in the solvent to give H_2O_2 and FAD to complete a catalytic cycle.[25] A number of LSD1 inhibitors with several chemotypes, including cyclopropyl-amine, propargylamine, hydrazine, and triazole dithiocarba-mate, have been reported in journals and patents,[26,27] as representatively shown in Figure 1B. Most LSD1 inhibitors are cyclopropylamine containing compounds, derived from tranyl-cypromine (1), an inhibitor of MAO-A and -B as well as an FDA-approved antidepression drug. Mechanistically, the α-C atom of the cyclopropyl ring of these compounds is oxidized, causing opening of the constrained ring followed by covalent
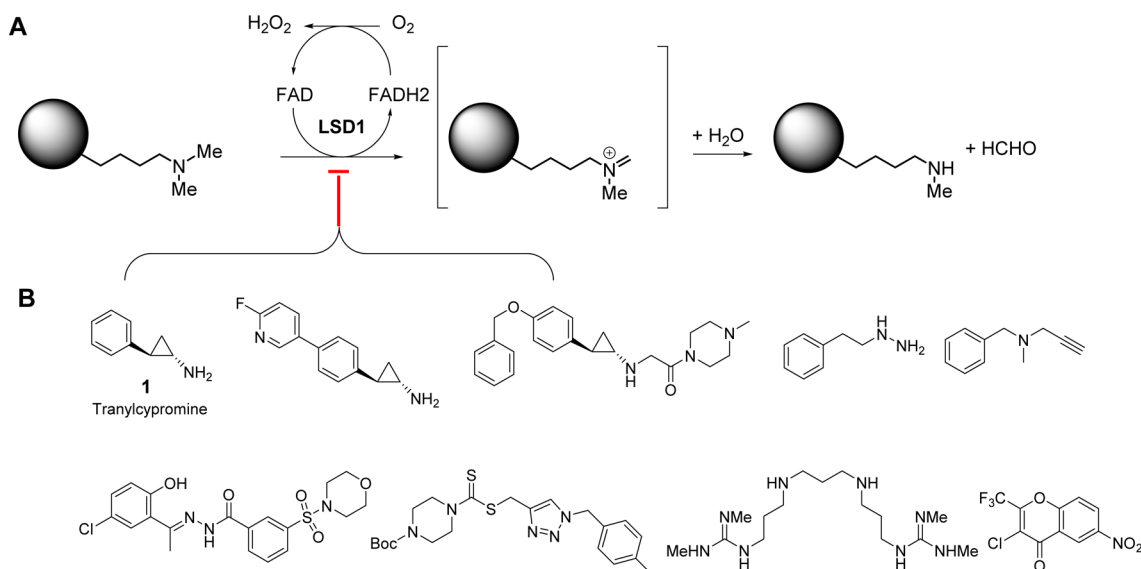
Figure 1. (A) Mechanism of catalysis for LSD1. (B) Structures of representative LSD1 inhibitors, among which compounds in the upper panel are irreversible inhibitors and those in the lower panel are reversible.

link to FAD (Supporting Information Figure S1).[25] Reversible LSD1 inhibitors have also been reported.[26b]
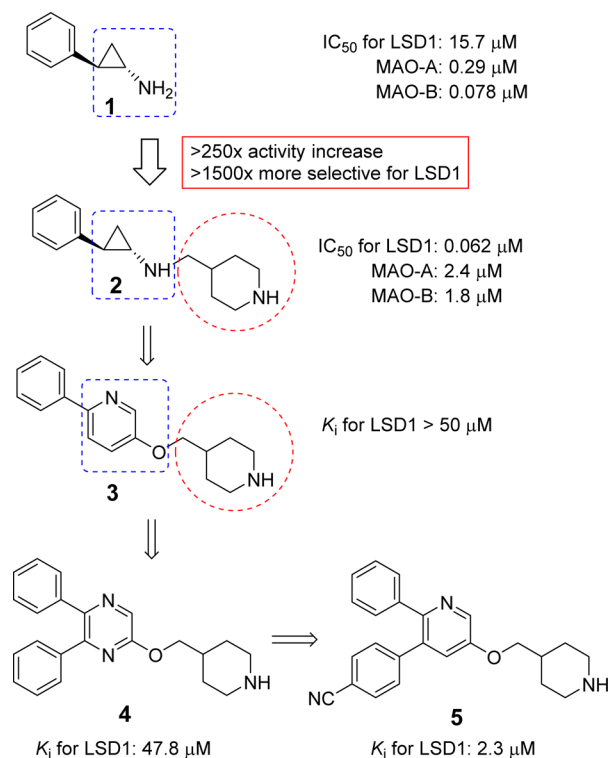
LSD1 has been suggested to be a drug target for several types of cancers (e.g., prostate and breast) due to its overexpression in these malignancies.[28−30] In addition, LSD1 was recently found to be required for an MLL-rearranged leukemia.[31] Knockdown of LSD1 can abrogate the transforming ability of the onco-MLL fusion gene and increase the H3K4me2 levels. Using a cyclopropylamine based LSD1 inhibitor also showed activity against the MLL-rearranged leukemia in cell and mouse models.[31] However, this compound was reported to have severe toxicities. Nonetheless, these previous studies have indicated LSD1 is a validated drug target and more chemotypes of inhibitors are therefore needed.[32,33]

Here, we report the discovery, synthesis, and structure–activity relationships (SARs) of 3-(piperidin-4-ylmethoxy)-pyridine containing compounds as potent LSD1 inhibitors. Enzyme kinetics and molecular modeling studies were used to investigate the possible mechanism of inhibition as well as the binding mode of these compounds. Molecular and cell biology experiments were performed to characterize the biological activities of selected compounds. During the revision of this manuscript, we noticed that scientists at GlaxoSmithKline found a structurally similar LSD1 inhibitor and presented its preliminary data at the 2013 American Association of Cancer Research annual meeting.[34,26b,27i]

■ RESULTS AND DISCUSSION

Inhibitor Design and Discovery. On the basis of the results from previous[27a] and our own studies on cyclopropyl-amine containing inhibitors of LSD1, it is clear that a second basic N-substituent, such as the piperidin-4-ylmethyl group (in red dashed circle, Chart 1) in compound **2**, can significantly increase the inhibitory activity as well as selectivity for LSD1. For example, compound **2** (IC$_{50}$ = 62 nM) is ∼250-fold more active against human recombinant LSD1 than compound **1** (IC$_{50}$ = 15.7 μM [31]) and, moreover, the piperidin-4-ylmethyl group enhances the enzyme selectivity for LSD1 by >1500-fold. Similar features have been observed by us and others[27a] for compounds **S1** and **S2** for the (4-methylpiperazin-1-yl)-

Chart 1. Inhibitor Design Leading to the Finding of New LSD1 Inhibitors[a]

IC$_{50}$ for LSD1: 15.7 μM
MAO-A: 0.29 μM
MAO-B: 0.078 μM

>250x activity increase
>1500x more selective for LSD1

IC$_{50}$ for LSD1: 0.062 μM
MAO-A: 2.4 μM
MAO-B: 1.8 μM

K_i for LSD1 > 50 μM

K_i for LSD1: 47.8 μM K_i for LSD1: 2.3 μM

[a]IC$_{50}$ values of compound **1** against MAO-A and -B are from ref 35.

carbonylmethyl group in compound **S2** (Supporting Information Figure S2). These data strongly support an important role of these basic amine groups in inhibitor recognition and/or binding to LSD1. However, there has been no structural information as to how these groups bind to LSD1, since X-ray crystallography might not be suited for this study because these groups are to be eliminated upon completion of the reaction (Figure S1). Nevertheless, given its important role in inhibitory potency and selectivity for LSD1, a basic amine group such as
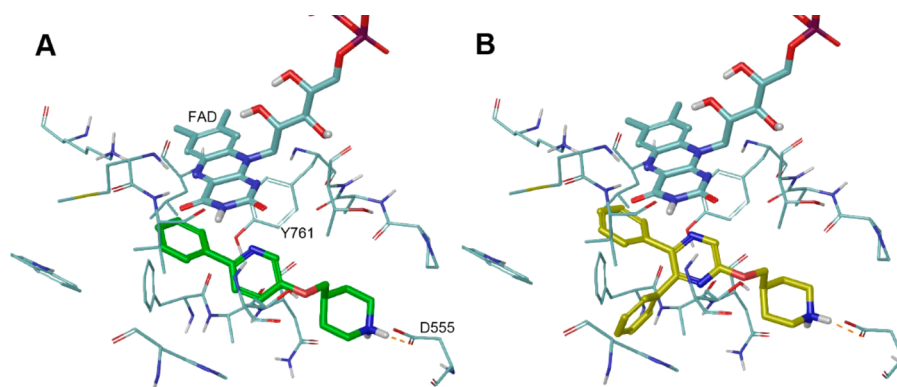
Figure 2. Docking studies of potential LSD1 inhibitors, using an LSD1 crystal structure (PDB code 2V1D) as the docking template. For clarity, only key residues (in light blue) in the active site of LSD1 are shown, together with the cofactor FAD (light blue tube model). Hydrogen bonds are shown as orange dashed lines. (A) Lwest-energy docking structure of compound **3** (tube model with C atoms in green), suggesting favorable interactions between its pyridine ring and FAD and Y761. (B) Lowest-energy docking structure of **4** (in yellow), showing introducing an additional 5-phenyl group could be favorable.

piperidin-4-ylmethyl should be included for the design of new LSD1 inhibitors.

We wished to find competitive, druglike inhibitors of LSD1 that do not covalently bind to FAD or the enzyme. Compound **3** (Chart 1) was designed in which the piperidin-4-ylmethyl and the phenyl group in the potent inhibitor **2** are retained, while the reactive cyclopropylamine moiety is replaced by a chemically stable pyridine core. Our modeling (docking) study (Figure 2A) predicted that the protonated piperidine amino group (at the physiological pH) could form a hydrogen bond with Asp555 and the pyridine ring could have favorable electrostatic and hydrophobic interactions with the flavin ring of FAD as well as Tyr761. Compound **3** was found to be inactive presumably due to the large active site of LSD1. Compound **4** was next designed with the rationale that an additional phenyl group could increase the binding affinity to LSD1, as suggested by docking (Figure 2B). The use of the pyrazine ring in **4** was intended for quick synthesis (see the Synthesis section below). Compound **4** was found to be a weak inhibitor with an apparent K_i value of 47.8 μM. We next performed a small scale of SAR studies (described below) based on compound **4**, which yielded a good inhibitor **5** with a K_i value of 2.3 μM. Enzyme kinetics studies (described below) suggested that compound **5** is a competitive inhibitor of LSD1 against a dimethylated H3K4 peptide substrate. These findings, together with its druglike chemical structure, show that compound **5** represents a promising new scaffold for further inhibitor optimization.

Synthesis. Scheme 1 illustrates a general method for synthesis of pyrazine containing inhibitors. A commercially available benzil compound was reacted with an equal molar amount of 2-aminoacetamide in the presence of sodium hydroxide to give 2-hydroxy-5,6-diphenylpyrazine. Upon treatment with POCl$_3$, its 2-hydroxy group was converted to a -Cl. The compound thus obtained was subjected to a substitution reaction using a sodium salt of *tert*-butyloxycarbonyl (BOC) protected 4-(hydroxymethyl)piperidine. Pyrazine containing inhibitors (such as compound **4**) were synthesized after deprotection of the BOC group. In addition, treatment of the BOC protected intermediate compound (R = Br) with zinc cyanide in the presence of a catalytic amount of Pd(PPh$_3$)$_4$ to produce a mixture of monocyano and dicyano substituted compounds, which can be carefully separated by column

**Scheme 1. General Synthetic Method for Pyrazine Containing Inhibitors**[a]
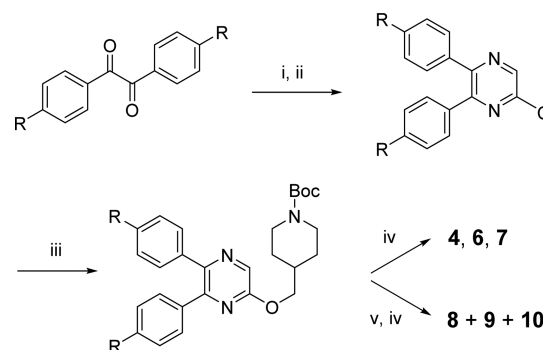
[a]Reagents and conditions: (i) 2-aminoacetamide, NaOH; (ii) POCl$_3$; (iii) BOC protected 4-(hydroxymethyl)piperidine, NaH; (iv) HCl in 1,4-dioxane; (v) Pd(PPh$_3$)$_4$, Zn(CN)$_2$.

chromatography to give, upon deprotection, compounds **8–10** (described below).

Scheme 2 shows a general synthesis of 3-(piperidin-4-ylmethoxy)pyridine containing LSD1 inhibitors (such as

Scheme 2. General Synthetic Method for Pyridine Containing Inhibitors[a]
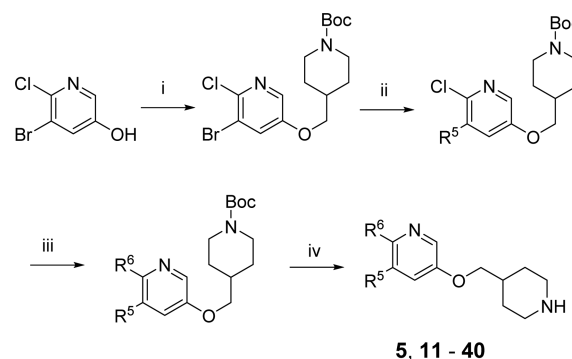
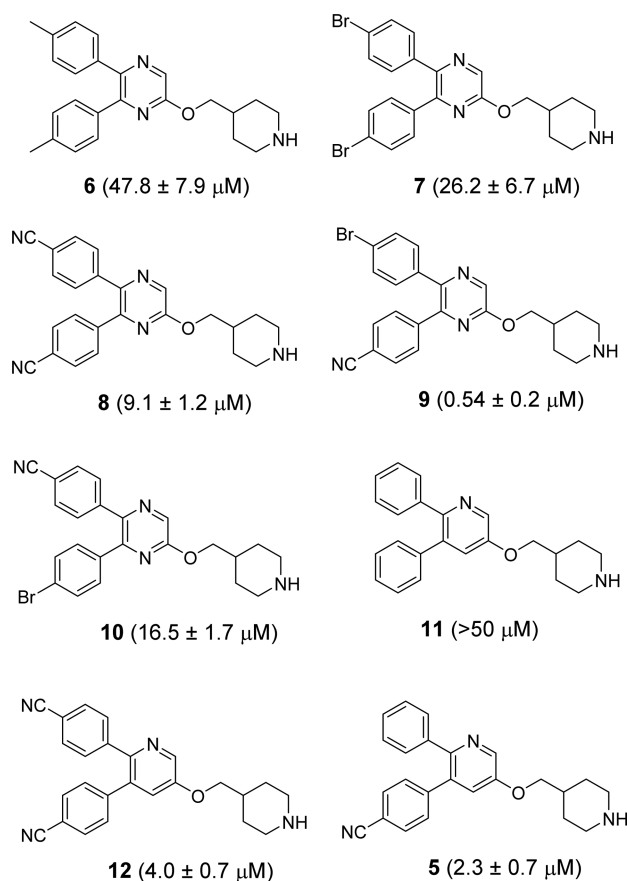[a]Reagents and conditions: (i) BOC protected 4-(hydroxymethyl)-piperidine, PPh$_3$, diisopropyl azodicarboxylate; (ii) R^5-B(OH)$_2$, Pd(PPh$_3$)$_4$, Na$_2$CO$_3$, 80 °C; (iii) R^6-B(OH)$_2$, Pd(PPh$_3$)$_4$, K$_3$PO$_4$, 140 °C; (iv) HCl in 1,4-dioxane.

C

compound **5**). A Mitsunobu reaction between 5-bromo-6-chloropyridin-3-ol and BOC protected 4-(hydroxymethyl)-piperidine introduces a BOC-protected 3-(piperidin-4-ylmethoxy) R[3] substituent. A selective Suzuki coupling reaction was performed to give R[5]-substituted compound, which underwent a second Suzuki coupling reaction with its 6-Cl group to add a R[6]-substituent. Upon deprotection of the BOC group, 3-(piperidin-4-ylmethoxy)pyridine containing compounds **5, 11−40** can be obtained. In addition, by use of similar methods, related compounds **41−45** can be readily synthesized (Supporting Information Experimental Section).

SAR Studies. Upon obtaining compound **4** with an apparent K_i value of 47.8 μM, we synthesized several analogs of **4** shown in Chart 2. Compound **6** with 5,6-di-(4-tolyl) and

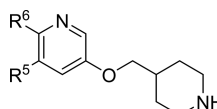**Chart 2. Structures and K_i Values (in Parentheses) of Compounds 5−12**

6 (47.8 ± 7.9 μM)

7 (26.2 ± 6.7 μM)

8 (9.1 ± 1.2 μM)

9 (0.54 ± 0.2 μM)

10 (16.5 ± 1.7 μM)

11 (>50 μM)

12 (4.0 ± 0.7 μM)

5 (2.3 ± 0.7 μM)

compound **7** with 5,6-di-(4-bromophenyl) substituents are more active (K_i = 32.2 and 26.2 μM, respectively), showing the two methyl or bromo groups are favorable. Synthesized from **7** using a Pd-catalyzed reaction, compound **8** with 5,6-di-(4-cyanophenyl) was found to be considerably more active with a K_i of 9.1 μM. In addition, monocyano substituted compounds **9** and **10** were also synthesized, which can be separated by column chromatography. One isomer **9** exhibited potent inhibitory activity against LSD1 with a K_i value of 540 nM, while the other isomer **10** (K_i = 16.5 μM) is less active than compound **8**. This indicated that 5- and 6-substituent in compounds **4, 6−10** should be individually optimized for LSD1 inhibition. However, this is not synthetically feasible for compounds with a pyrazine core.
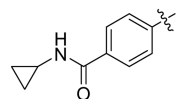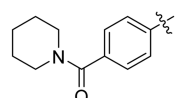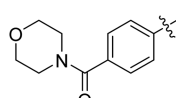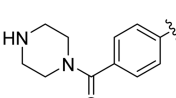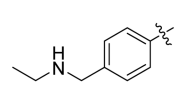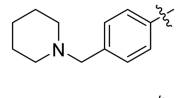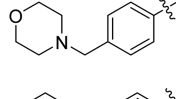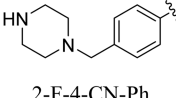
The pyridine core structure, in which the two substituents can be modified separately, was used for SAR studies. Although compound **11** (Chart 2, which corresponds to the pyrazine compound **4**) is inactive, compound **12** with a K_i value of 4.0 μM is a good LSD1 inhibitor and stronger than the corresponding pyrazine compound **8**. This showed the pyridine core can be a good scaffold for activity optimization.

The 6-position of the pyridine ring was optimized, and the results are summarized in Table 1. Compound **5** with an unsubstituted 6-phenyl group was found to be slightly more active (K_i = 2.3 μM) than **12**. Compound **13** having a 4-fluorophenyl group exhibited potent inhibitory activity with a K_i of 220 nM, ∼10× more active than the parent compound **5**. Adding an additional -F at the 3- or 2-position in compound **14** (K_i = 570 nM) or **15** (K_i = 1.2 μM), respectively, resulted in a ∼2.5× or 5.5× activity reduction, suggesting that 3- or 2-substitution of the phenyl ring seems to be disfavored. The 4-trifluoromethyl group in compound **16** considerably enhanced the inhibitory potency to 58 nM. Change to a 4-methyl group in compound **17** (K_i = 29 nM) further caused a ∼2-fold activity increase. Move of the methyl group to 3-position in compound **18** (K_i = 800 nM) drastically decreased the activity by ∼27-fold, showing again substitution at the 4-position of the 6-phenyl ring is favorable. Compounds **19** and **20** with a 4-ethyl and 4-isopropyl group, respectively, were found to be ∼7× and 3× less active (K_i = 200 and 88 nM) than **17** with a 4-methyl, showing a bigger alkyl group at this position is less favorable. As compared to the most potent inhibitor **17**, while compound **21** (K_i = 740 nM) having a 4-methoxy group showed a significant activity reduction, compound **22** with a 4-trifluoromethoxy substituent exhibited a similar inhibitory activity (K_i = 46 nM). Activities of compounds **23−26** indicated that a 6-pyridinyl ring is less favorable than a phenyl ring. Compounds **23** and **24** (K_i = 5.0 and 3.2 μM) with a pyridin-4-yl and -3-yl ring, respectively, are slightly less active than is compound **5** (K_i = 2.3 μM). More noticeably, compound **25** (K_i = 1.8 μM) with a 4-fluoropyridin-3-yl substituent exhibited a ∼8-fold activity reduction as compared to the corresponding phenyl compound **13**. Although the 4-methyl group in compound **26** resulted in a significant activity increase (K_i = 380 nM, as compared to 3.2 μM for compound **24**), compound **26** is still ∼13× less active than the corresponding phenyl compound **17**. In addition, introducing a 3-thiophenyl ring to the 6-position produced compound **27**, which exhibited a comparable inhibitory activity (K_i = 2.4 μM) to that of the phenyl compound **5**.

Next, compounds **28−40** were synthesized and tested for LSD1 inhibition for SAR studies of the 5-position of the most potent inhibitor **17**. As summarized in Table 1, the 4-cyano substituent of the 5-phenyl ring has turned out to be critically important for LSD1 inhibition. Compound **28** with a 4-ethynyl group was surprisingly found to suffer from a complete (>1700×) activity loss, despite a similar size of the R[5] groups. This could be due to different electrostatic properties between the ethynyl (in **28**) and the cyano group (in **17**). Compounds **29** and **30** with a 4-carboxy and 4-hydroxymethyl group in the 5-phenyl ring also completely lost inhibitory activities. In addition, compounds **31−34**, which contain a 4-amide group with a range of steric, hydrophobic, and electronic properties, were found to be inactive. Compounds **35−38** having a 4-aminomethyl group retained some inhibitory activities against LSD1. Compound **35** with a smaller ethylaminomethyl group is a weak inhibitor with a K_i of 22.3 μM, while compounds **36** and **37** having a bulkier piperidin-1-ylmethyl and morpholin-4-

Table 1. Structures and Activity of Compounds 5, 12−40

|	R^5	R^6	K_i (μM)		R^5	R^6	K_i (μM)
5	4-CN-Ph	Ph	2.3 ± 0.7	31	cyclopropylcarbamoyl-Ph (N-cyclopropyl benzamide)	4-Me-Ph	>50
12	4-CN-Ph	4-CN-Ph	4.0 ± 0.7	32	piperidin-1-ylcarbonyl-Ph	4-Me-Ph	>50
13	4-CN-Ph	4-F-Ph	0.22 ± 0.07	33	morpholin-4-ylcarbonyl-Ph	4-Me-Ph	>50
14	4-CN-Ph	3,4-di-F-Ph	0.57 ± 0.09	34	piperazin-1-ylcarbonyl-Ph	4-Me-Ph	>50
15	4-CN-Ph	2,4-di-F-Ph	1.2 ± 0.6	35	ethylaminomethyl-Ph	4-Me-Ph	22.3 ± 1.4
16	4-CN-Ph	4-CF$_3$-Ph	0.058 ± 0.022	36	piperidin-1-ylmethyl-Ph	4-Me-Ph	>50
17	4-CN-Ph	4-Me-Ph	0.029 ± 0.018	37	morpholin-4-ylmethyl-Ph	4-Me-Ph	43.8 ± 5.7
18	4-CN-Ph	3-Me-Ph	0.80 ± 0.21	38	piperazin-1-ylmethyl-Ph	4-Me-Ph	7.6 ± 2.1
19	4-CN-Ph	4-Et-Ph	0.20 ± 0.06	39	2-F-4-CN-Ph	4-Me-Ph	0.22 ± 0.13
20	4-CN-Ph	4-*i*-Pr-Ph	0.088 ± 0.033	40	3-F-4-CN-Ph	4-Me-Ph	0.15 ± 0.03
21	4-CN-Ph	4-OMe-Ph	0.74 ± 0.04				
22	4-CN-Ph	4-OCF$_3$-Ph	0.046 ± 0.011				
23	4-CN-Ph	Pyridin-4-yl	5.0 ± 0.6				
24	4-CN-Ph	Pyridin-3-yl	3.2 ± 0.7				
25	4-CN-Ph	4-F-Pyridin-3-yl	1.8 ± 0.6				
26	4-CN-Ph	4-Me-Pyridin-3-yl	0.38 ± 0.1				
27	4-CN-Ph	3-thiophenyl	2.4 ± 0.7				
28	4-ethynyl-Ph	4-Me-Ph	>50				
29	4-HO$_2$C-Ph	4-Me-Ph	>50				
30	4-(HOCH$_2$)-Ph	4-Me-Ph	>50				

ylmethyl substituent, respectively, are almost inactive. Interestingly, compound **38** with a dibasic piperazin-1-ylmethyl group is a fairly good inhibitor with a K_i of 7.6 μM, although it is >250× less active than compound **17** having the corresponding -CN substituent. Moreover, compared to **17**, adding a -F into the 2- and 3-position of the 5-phenyl ring in compounds **39** and **40** (K_i = 220 and 150 nM), respectively, resulted in ~8× and 5× activity reductions.

Finally, several compounds shown in Chart 3 were synthesized for the SAR study of the 3-(piperidin-4-ylmethoxy)pyridine core structure. Compound **41** (K_i = 4.9 μM) with a benzene core structure is ~170-fold less potent than compound **17**, suggesting the pyridine core is of importance for the activity. Although it is a racemic mixture, the 650 nM K_i value of compound **42** shows that the piperidin-3-yl substituent is significantly less favorable than the piperidin-4-yl group in **17**. Greatly reduced activity of compound **43** (K_i = 1.2 μM) also indicates that change of an -O- linkage in compound **17** to a -NH- is highly disfavored. Loss of activity for compounds **44** (with a 3-OH group) and **45** (with a 3-

benzyloxy group) clearly shows the critical role of the basic piperidine side chain in LSD1 inhibition.

Enzyme Kinetics Studies. A steady-state enzyme kinetics study of compound **5**, which is a representative compound for this novel series of LSD1 inhibitors, was performed to determine the possible mechanism of action. Since the cofactor FAD has a very high affinity to LSD1, as evidenced by its presence in the enzyme even after a lengthy expression and purification process, the kinetics study was performed against a dimethylated H3K4 peptide substrate with a sequence of ARTK(Me2)QTARKSTGGKAPRKQKA. Initial velocities of the LSD1 catalyzed reaction were measured with increasing concentrations of compound **5** and the substrate. The program SigmaPlot was used for enzyme kinetics modeling. The reaction rate and ligand concentration data were imported into the program and fitted to either competitive, uncompetitive, or noncompetitive inhibition models. The best model, as judged by R^2 and AICc values, would show the mode of action for the inhibitor. Thus, compound **5** was found to be a competitive inhibitor of LSD1 against the substrate because the kinetics

Chart 3. Structures and K_i Values (in Parentheses) of Compounds 41−45

41 (4.9 ± 1.0 μM)

42 (0.65 ± 0.20 μM)

43 (1.2 ± 0.31 μM)

44 (>50 μM)

45 (>50 μM)
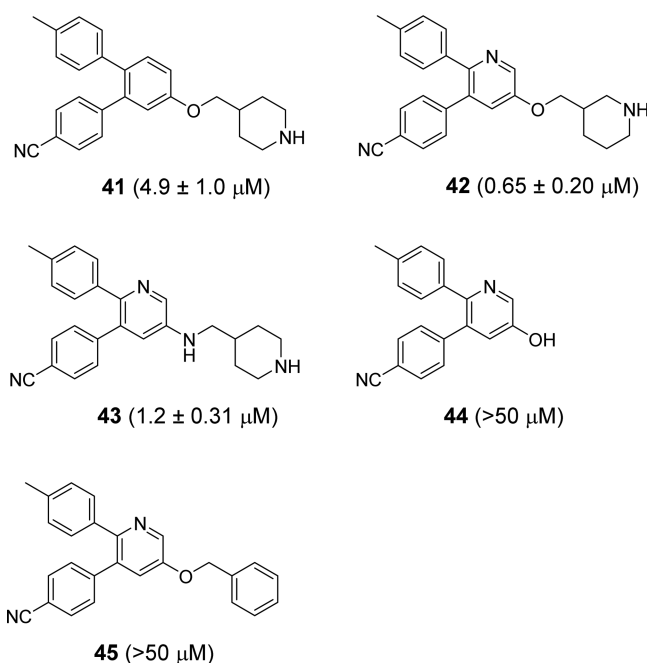
data for **5** were best fitted to the competitive mode of action (Figure 3), as compared to the uncompetitive and noncompetitive fitting (Figure S3).

Docking Studies. We carried out molecular modeling (docking) studies to predict how the most potent inhibitor **17** binds to LSD1. A number of X-ray crystal structures of LSD1 in complex with covalent inhibitors,[25,36] a reversible inhibitor,[37] and substrate-like peptide[38,39] are available for the study. The docking program Glide in Schrödinger Suite molecular modeling software package was used for docking.[40] The crystal structure (PDB code 2V1D) of human LSD1 in complex with a H3K4 mimetic peptide[39] (with a K4M mutation) was used as a docking template, which was prepared by adding hydrogen atoms to the structure, removing the peptide and water molecules, while keeping FAD as an integrated component of the protein. Compound **17** can be well docked into the active site of LSD1, with its 20 docking structures with the lowest

energies tightly clustered to one another and having similar binding features (Figure 4A). The pyridine core, tolyl (R^6), 4-cyanophenyl (R^5), and piperidin-4-ylmethoxy (R^3) groups of these 20 structures are located in the same site or pocket in LSD1. Figure 4B and Figure 4C show two views of the binding conformation of **17** with the lowest docking energy in the active site of LSD1. Its central pyridine ring is predicted to have favorable hydrophobic as well as electrostatic interactions with the flavin ring, Tyr761, Ala809, Thr810, and Ala539. The tolyl R^6 group was found to be located in a mostly hydrophobic pocket surrounded by flavin, Phe538, Val333, Tyr761, Met332, Leu659, Lys661, and Trp695. The 4-cyanophenyl R^5 group occupies a pocket surrounded by with Ala539, Phe538, Trp695, His564, and Thr335 and has favorable interactions with these residues. The protonated amine of the piperidin-4-ylmethoxy group was found to have a hydrogen bond as well as electrostatic interactions with the negatively charged side chain of Asp555. In addition, the skeleton of the piperidin-4-ylmethoxy group possesses hydrophobic interactions with Ala809, Pro808, Ala539, and Asn540.

Of interest is that the docking results could be used to rationalize our experimental SAR. For example, the predicted strong interactions between the protonated piperidin-4-ylmethoxy group and Asp555 (Figure 4B) could explain the importance of this group for LSD1 inhibition. As comparof ied to compound **41** with a benzene core structure, possibly enhanced interactions between the pyridine core in **17** and flavin as well as Tyr761 (Figure 4B) could account for the increased activity of **17**. For SAR on the R^6 group, as compared to compound **5**, the increased activity of **17** could be due to the favorable interactions of the methyl group in **17** with Phe538, Val333, Met332, and Lys661 (Figure 4B and Figure 4C). In addition, the methyl is predicted to range from ∼3.3 Å away from Met332 to ∼4.8 Å from Trp695 by the docking study. This limited space might account for somewhat decreased activities of compounds **19** and **20** with a bigger -Et and -*i*-Pr group, respectively.

Enzyme Selectivity. LSD1 belongs to a family of FAD-dependent monoamine oxidases including MAO-A and -B. Due to an important role of MAO-A and -B in degradation of neurotransmitters in the central nervous system, selective inhibition of LSD1 is highly desirable. We investigated enzyme selectivity of several representative 3-(piperidin-4-ylmethoxy)-
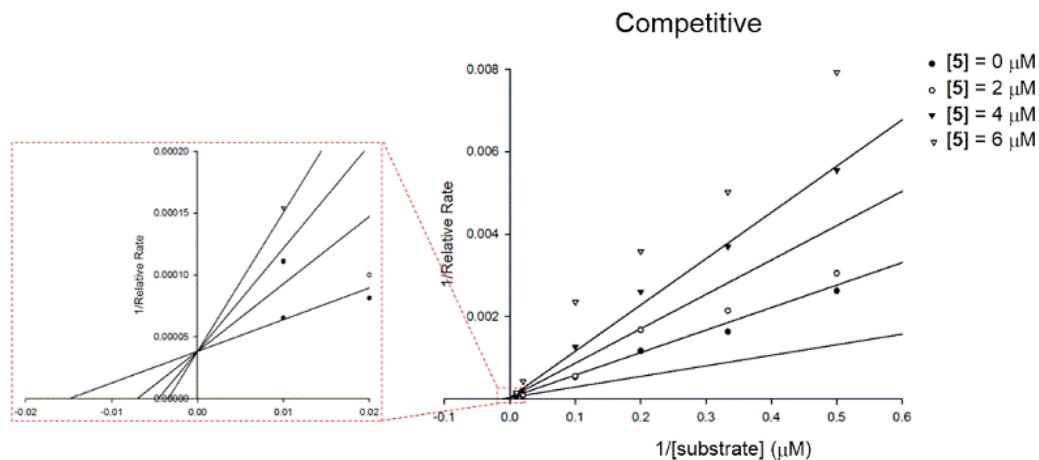
Figure 3. Lineweaver−Burk plot of competitive inhibition model for compound **5** with variable concentrations of the dimethylated H3K4 peptide substrate, with an enlarged figure in the left panel showing details near the origin. The K_i was determined to be 1.8 μM in this experiment.
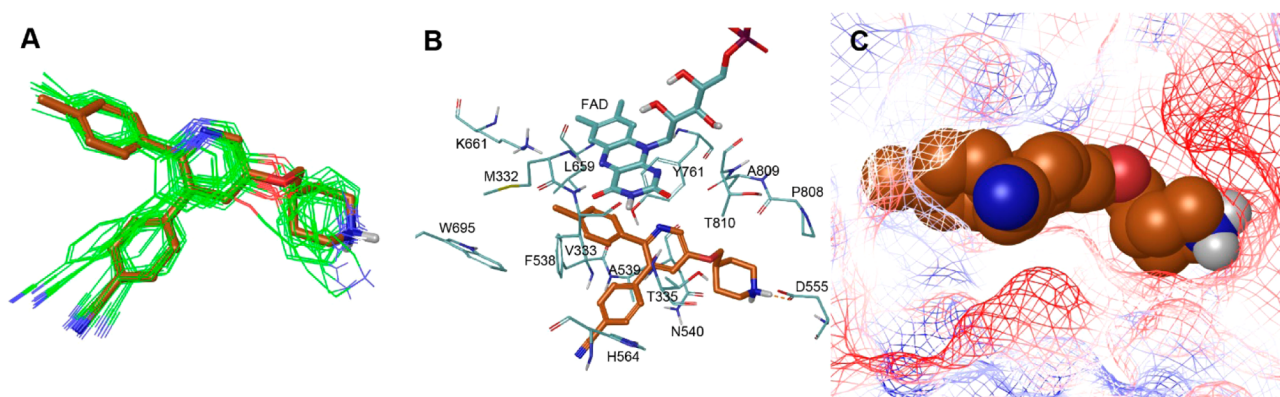
Figure 4. Docking results of compound **17**, using an LSD1 structure (PDB code 2V1D) as the docking template: (A) 20 lowest-energy docking structures of compound **17**, with the most stable conformation shown as an orange tube model; (B) lowest-energy docking structure of **17**, showing the interacting key residues (in light cyan) of LSD1 and FAD (light cyan tube model); (C) lowest-energy docking structure of **17** (as a space-filing model) in the active site of LSD1 (shown as a meshed electrostatic potential surface model).

pyridine containing LSD1 inhibitors against MAO-A and -B. Thus, compounds **5**, **16**, **17**, and **22** were tested for their activity against recombinant human MAO-A and -B and their selectivity indices were also calculated. These results are summarized in Table 2. All four potent LSD1 inhibitors did

Table 2. Inhibitory Activity (K_i, μM) against MAO-A and -B and Selectivity Index for LSD1

compd	LSD1	MAO-A	MAO-B	selectivity index
5	2.3	>50	10.6 ± 2.8	>4.6
16	0.058	>50	9.7 ± 2.9	>160
17	0.029	>50	18.7 ± 6.9	>640
22	0.046	>50	2.6 ± 1.2	>56

not significantly inhibit MAO-A with K_i > 50 μM, showing excellent selectivity. For MAO-B, compounds **5**, **16**, and **17** had only weak activities with K_i values of 9.7−18.7 μM. Due to its relatively low activity against LSD1, compound **5** showed 4.6× selectivity against MAO-B. However, potent LSD1 inhibitors **16** and **17** exhibited very high selectivity of >160- and >640-fold against MAO-B, respectively. Moreover, despite having a relatively good activity against MAO-B (K_i = 2.6 μM), compound **22** is still a highly selective LSD1 inhibitor with a selectivity index of >56 against MAO-B, because of its potent inhibition of LSD1. Structurally, the 4-CF_3, -Me, and -OCF_3 of the 6-phenyl ring in compounds **16**, **17**, and **22**, respectively, account for the high selectivity against MAO-B because as compared to the parent compound **5**, these substituents have less impact (<4×) on MAO-B inhibition but increase the inhibitory potency against LSD1 by >39-fold.

Structurally similar 5,6-diaryl-3-(aminoalkyloxy)pyridine compounds were reported to be potent inhibitors of Akt kinase,[41] which is also a drug target for cancer. We examined the enzyme selectivity of the most potent compound **17** against human Akt. Compound **17** was found to have a weak activity against Akt with an IC_{50} value of 87.6 ± 21.6 μM, showing a high enzyme selectivity for LSD1. In addition, these compounds were reported as nicotinic receptor ligands[42] as well as antituberculosis agents.[43] Although these do not directly relate to the antitumor purpose of this study, a comprehensive enzyme selectivity profiling could be useful for future development of these compounds.

Cell Activity Testing. The most potent compound **17** was tested to see whether it can change the cellular H3K4 methylation level in a leukemia cell line MV4-11. Thus, cells were treated with **17** at 0.2 and 1 μM and histones were then collected, separated by electrophoresis, and probed by a specific antibody of H3K4me2, as well as that of histone H3 as input controls. As can be seen in Figure 5, compound **17** appeared to
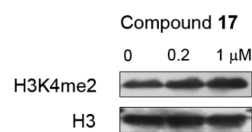
Figure 5. Treatment of MV4-11 cells with potent LSD1 inhibitor **17** caused an increased cellular level of H3K4me2.

increase the cellular level of H3K4me2 at 1 μM, suggesting it is cell membrane permeable and inhibits LSD1 in cells. It is noted because this method is semiquantitative. More quantitative investigation could be useful to characterize how compound **17** affects cellular histone methylations globally and at specific gene loci.

Next, selected potent LSD1 inhibitors, including compound **S2** (which is a cyclopropylamine-containing inhibitor, Figure S2) as a positive control, were tested for their ability to inhibit proliferation of four tumor cell lines and a normal fibroblast cell line WI-38. Among the four tumor cells, MV4-11 and Molm-13 are leukemia cell lines with an MLL gene translocation. Two representative breast cancer cells MCF-7 (estrogen receptor positive) and MDA-MB231 (estrogen receptor negative) were also included in the study, since LSD1 is often overexpressed in breast cancers. The results are summarized in Table 3, together with the LSD1 inhibitory activity of these compounds. Of interest is that the five competitive inhibitors exhibited strong antitumor activities against the four tumor cells with EC_{50} values of 280 nM to 8.6 μM. However, these compounds had weak or no activity against the growth of normal fibroblast cells WI-38. Particularly, LSD1 inhibitors **16**, **17**, **20**, and **22** showed potent activity against proliferation of MV4-11 leukemia cells with EC_{50} values ranging from 280 nM to 480 nM, while less potent compound **13** exhibited a reduced activity (EC_{50} = 1.1 μM). These compounds were also found to have strong activity against the growth of Molm-13 leukemia cells with EC_{50} values of 0.84−4.4 μM. For MCF-7 breast cancer, more potent LSD1

Table 3. Antiproliferative Activity (EC$_{50}$, μM) of LSD1 Inhibitors against Cancer and Normal Cells

compd	LSD1 K_i (μM)	MV4-11	Molm-13	MCF-7	MDA-MB231	WI-38
13	0.22	1.1 ± 0.12	4.4 ± 1.1	6.9 ± 1.8	8.6 ± 2.4	>50
16	0.058	0.28 ± 0.03	0.84 ± 0.18	3.6 ± 1.5	6.9 ± 1.9	30.0 ± 9.2
17	0.029	0.36 ± 0.13	3.4 ± 1.2	3.6 ± 1.5	5.6 ± 1.0	26.6 ± 6.9
20	0.088	0.30 ± 0.02	3.2 ± 1.1	3.3 ± 0.8	7.6 ± 2.9	20.0 ± 4.6
22	0.046	0.48 ± 0.12	3.6 ± 0.5	5.3 ± 2.2	7.5 ± 2.2	17.5 ± 4.8
S2	0.077[a]	0.084 ± 0.026	0.32 ± 0.1	6.6 ± 2.0	8.9 ± 2.5	>50

[a]IC$_{50}$ value for compound **S2**, which is a covalent inhibitor of LSD1.

inhibitors **16**, **17**, **20**, and **22** appeared to be superior (EC$_{50}$ of 3.3−3.6 μM) to compound **13** (EC$_{50}$ of 6.9 μM). These compounds also showed fairly good antiproliferative activity against MDA-MB231 breast cancer cells with EC$_{50}$ values of 5.6−8.6 μM. In addition, these five competitive LSD1 inhibitors showed similar antitumor activities as compared to the covalent inhibitor **S2**, which also exhibited strong antiproliferative activity (EC$_{50}$ of 0.084−8.9 μM) against the tumor cells, while it was inactive against the normal cells. Overall, the strong and selective antitumor activity suggested that this class of LSD1 inhibitors could be potentially useful cancer therapeutics and further efforts of compound development are therefore warranted.

CONCLUSIONS

LSD1 plays an important role in maintaining a balanced methylated H3K4, a key "histone code" for active gene transcription. It has also been found to be overexpressed in certain cancers such as breast cancer.[28−30] Therefore, LSD1 represents a drug target for intervention and more chemotypes of potent LSD1 inhibitors are needed.

On the basis of previous SAR of cyclopropylamine containing LSD1 inhibitors, a series of 3-(piperidin-4-ylmethoxy)pyridine and related compounds were found to be new LSD1 inhibitors. Structure guided molecular modeling and medicinal chemistry studies have led to the identification of several potent LSD1 inhibitors (e.g., **16**, **17**, **20**, and **22**) with K_i values as low as 29 nM. SAR investigation of this series of compounds showed that (1) a pyridine or pyrazine core structure is superior to a benzene ring; (2) a basic 3-(piperidin-4-ylmethoxy) R^3 group is important to LSD1 inhibition; (3) 4-cyanophenyl group is the best R^5 substituent in this study, while many other groups such as amide or alkyl-containing phenyl groups significantly reduce the inhibitory activity; (4) a phenyl R^6 group is superior to a corresponding pyridine group; and (5) among the substituted phenyl R^6 groups, several para-substituents (e.g., -Me, CF$_3$, and -OCF$_3$ in **17**, **16**, and **22**) can significantly enhance LSD1 inhibition (by as high as 79×), while meta- or ortho-substituents are less effective.

Enzyme kinetics studies suggested that these compounds are competitive inhibitors against the dimethylated H3K4 peptide substrate. Consistent with the kinetics data, docking studies showed that these compounds can be well docked into the substrate binding site of LSD1. In addition, the docking results could be used to rationalize many of the observed SARs. Several representative LSD1 inhibitors were found to exhibit very high selectivity against related MAO-A and -B enzymes. This feature is desirable for this series of LSD1 inhibitors, due to important functions of MAO-A and -B in the central nervous system. The most potent LSD1 inhibitor **17** was found to increase the cellular level of H3K4me2, showing on-target activity in cells. However, it did not significantly affect the

methylation levels of several other histone lysine residues (including H3K4me3), presumably because these are not cellular substrates of LSD1. Finally, five potent LSD1 inhibitors were found to exhibit potent to good activity against proliferation of two MLL-rearranged leukemia cells and two breast cancer cells with EC$_{50}$ values ranging from 0.28 to 8.6 μM, while no or very weak activity of these compounds against the growth of normal fibroblast cells was observed.

EXPERIMENTAL SECTION

All chemicals for synthesis were purchased from Alfa Aesar (Ward Hill, MA) or Aldrich (Milwaukee, WI). All compounds were characterized by ^{1}H NMR on a Varian (Palo Alto, CA) 400-MR spectrometer. Identification of the most active compounds was confirmed by HRMS using an Agilent 6550 iFunnel quadrupole-time-of-flight (Q-TOF) mass spectrometer with electrospray ionization (ESI). The purities of synthesized compounds were determined by a Shimadzu Prominence HPLC with a Zorbax C18 column (4.6 mm × 250 mm) monitored by UV at 254 nm. The purities of the reported compounds were found to be >95%. HPLC−MS experiments were performed using a Shimadzu Prominence HPLC connected to a LCMS-2020 MS system.

Synthesis and characterization of compounds 4−45 can be found in Supporting Information Experimental Section.

LSD1 Inhibition. The catalytic domain (172−833) of human LSD1 was cloned, inserted into pGEX-KG vector, and the DNA sequence was verified by sequencing. The pGEX-KG-LSD1 plasmid thus generated was transformed into *E. coli* BL21-CodonPlus strain (Agilent) and cultured at 37 °C in LB medium containing ampicillin (50 μg/mL) and chloramphenicol (34 μg/mL). When the optical density of the bacterial culture approached ∼0.9 at 600 nm, LSD1 expression was induced by adding 0.2 mM isopropylthiogalactoside (IPTG) at 25 °C for 20 h. Cells were next collected, lysed, centrifuged for 20 min at 20 000 rpm. The resulting supernatant was subjected to an affinity column chromatography with glutathione sepharose resins. The recombinant GST-LSD1 fusion protein was obtained in ∼90% purity (SDS−PAGE) by elution with 10 mM glutathione solution and a secondary purification using a Superdex 200 gel filtration column chromatography followed by concentration.

A mass spectrometry based biochemical assay for LSD1 was developed, with the amount of demethylated product peptide being quantitatively determined by HPLC−MS. Increasing concentrations of a compound were incubated with LSD1 (150 nM) in 50 mM phosphate buffer (pH = 7.0) containing 0.01% Brij-35 for 10 min at 25 °C, before initiation of the reaction by adding 10 μM of dimethylated peptide substrate ARTK(Me2)QTARKSTGGKAPRKQKA. The total volume of the reaction mixture was 60 μL. Reactions were terminated after 30 min by adding 6 N formic acid (5 μL), and 20 μL of the reaction mixture was subjected to HPLC−MS to separate and determine the amount of the reaction product. HPLC was run using a Phenomenex C18 column (250 mm × 4.6 mm, 5 μm) with acetonitrile/water (40:60, containing 0.1% TFA) as an eluent at a flow rate of 0.5 mL/min. A selected ion monitoring (SIM) for 1142 Da was used to detect and quantitate the amount of the product ARTK(Me1)QTARKSTGGKAPRKQKA (parameters: interface voltage, 3.0 kV; detector voltage, 1.3 kV; nebulizing gas, 1.5 L/min; drying gas, 15 L/min; desolvation line temperature, 300 °C; heat block

temperature, 300 °C; Pirani gauge vacuum, 150 Pa; ion gauge vacuum: 5×10^{-4} Pa). To ensure an initial velocity was determined, ∼5% of the dimethylated substrate was consumed before the reaction was stopped. Therefore, monomethylated peptide was obtained almost as the only product. No significant amount of the nonmethylated product was detected.

Data were imported into Prism 5.0 (GraphPad), and the IC_{50} values were determined using the sigmoidal dose response fitting in the program. For compounds with $IC_{50} > 1.5$ μM (i.e., ≫[LSD1]), K_i values were calculated using the Cheng−Prusoff equation $K_i = IC_{50}/(1 + [S]/K_m)$, where [S] is the concentration of the peptide substrate (10 μM) and K_m is a reported value of 10 μM.[27a] For compounds with $IC_{50} < 1.5$ μM, K_i values were calculated using the Morrison tight inhibition modeling in Prism. The reported K_i values were the mean values of at least three independent experiments.

Enzyme Kinetics Study. A steady-state kinetics study was conducted by measuring the initial velocities of reactions catalyzed by LSD1 while varying the concentrations of compound **5** (0, 2 μM, 4 μM, and 6 μM) and the peptide substrate (2 μM, 3 μM, 5 μM, 10 μM, 50 μM, and 100 μM). Data were imported into SigmaPlot and fitted into the competitive, noncompetitive, and uncompetitive inhibition models. The best kinetic model was determined by the highest R^2 and lowest AICc values. Lineweaver−Burk plots were generated by SigmaPlot.

Molecular Modeling. Docking studies were performed with our previous published methods[44−46] using Schrödinger suite (version 2015),[40] which includes all of the programs described below. The crystal structure of LSD1 in complex with an H3K4 peptide (PDB code 2V1D) was prepared using the module "Protein Preparation Wizard" in Maestro (version 10.1) using the default protein parameters. Hydrogen atoms were added, the H3K4 peptide ligand and all water molecules were extracted, and FAD was retained in the protein structure for docking. H-bonds were next optimized, the partial charges for all atoms were assigned, and the protein was energy-minimized using OPLS-2005 force field. A receptor grid, which is large enough to contain the active site, was generated with the program Glide without any constraints. Inhibitor compounds were built, energy-minimized using OPLS-2005 force field in Maestro, and then docked into the prepared protein structure using Glide (docking parameters: standard-precision and dock flexibly).

Inhibition of MAO-A/-B. Human recombinant MAO-A and -B enzymes were purchased from Sigma, and their biochemical activity and inhibition were determined using a MAO-Glo assay kit from Promega. Following the manufacturer's protocol, the assays were performed in 384-well white plates by adding all reagents in the kit, MAO-A or -B (100 nM) and increasing concentrations of inhibitors to a final volume of 20 μL. After 60 min, the reactions were stopped by adding a reconstituted luciferin detection reagent (20 μL/well). Upon incubation for an additional 20 min, luminescence of each well was determined using a Beckman DTX-880 microplate reader. Using K_m values provided in the kit, K_i values were similarly calculated as described above.

Inhibition of Akt Kinase. The inhibitory activity of compound **17** against human recombinant Akt kinase was determined using a commercially available ELISA kit (Enzo life Sciences, Farmingdale, NY). Following the manufacturer's protocol, Akt kinase (5 nM), ATP, and increasing concentrations of **17** (0.01−100 μM) were added to a final volume of 30 μL in a 96-well plate precoated with a substrate. After a 60 min incubation in 30 °C, the reactions were stopped by removal of all reactants. The primary antibody against the phosphorylated substrate and a peroxidase conjugated secondary antibody were added sequentially. The optical absorbance at 450 nM of each well was developed with tetramethylbenzidine substrate (TMB) and determined using a Beckman DTX-880 microplate reader. The data were imported into Prism (version 5.0, GraphPad) and IC_{50} values were calculated by using a standard dose response curve fitting. The reported value is the average of three independent experiments.

Western Blot. 10^6 MV4-11 cells/well were incubated with compounds **17** and **28** at 0.2 and 1 μM for 3 days. Histone proteins were extracted using EpiQuik total histone extraction kit (Epigentek)

according to the manufacturer's protocol. Equal amounts of histones (2 μg) were separated on SDS−PAGE and transferred to PVDF membranes. The blots were probed with primary antibodies against H3K4me2 and -me3, H3K27me2, H3K36me2, H4K20me2, and H3 (Cell Signaling), followed by anti-rabbit IgG (Thermo Scientific) secondary antibodies. Quantitation of these blots were performed using the program ImageJ.

Cell Growth Inhibition. The antiproliferation assays were done using our previous method.[47,48] In brief, for leukemia cells, 10^6 cells per well were added into 96-well plates and cultured with increasing concentrations of a compound in RPMI-1640 medium supplemented with 10% fetal bovine serum and penicillin (100 U/mL) and streptomycin (100 μg/mL) at 37 °C in a 5% CO_2 atmosphere with 100% humidity. For solid tumor and normal cells, 10^5 cells per well were added into 96-well plates and cultured in Dulbecco's modified Eagle medium (DMEM) supplemented with 10% fetal bovine serum and penicillin (100 U/mL) and streptomycin (100 μg/mL) overnight for cell attachment. After addition of increasing concentration of a compound, plates were incubated for a given period of time. Cell viability was assessed by using an XTT assay kit (Roche) for leukemia cells or an MTT assay (Sigma) for attachment cells. Compound IC_{50} values were calculated from dose response curves using Prism 5.0.

ASSOCIATED CONTENT

Ⓢ Supporting Information

The Supporting Information is available free of charge on the ACS Publications website at DOI: 10.1021/acs.jmedchem.5b01361.

> Figures S1−S3 and Experimental Section showing detailed compound synthesis and characterization (PDF)
> Molecular formula strings (CSV)

AUTHOR INFORMATION

Corresponding Author
*Phone: 713-798-7415. E-mail: ysong@bcm.edu.

Author Contributions
§F.W. and C.Z. contributed equally.

Notes
The authors declare no competing financial interest.

ACKNOWLEDGMENTS

ABBREVIATIONS USED

BOC, *tert*-butyloxycarbonyl; FAD, flavin adenine dinucleotide; H3K4, histone H3 lysine 4; H3K4me1, -2, or -3, mono-, di-, or trimethylated H3K4; LSD1, lysine specific demethylase 1; MAO, monoamine oxidase; MLL, mixed lineage leukemia; SAR, structure−activity relationship

REFERENCES

(1) For a recent review, see the following: Kouzarides, T. Chromatin modifications and their function. *Cell* **2007**, *128*, 693−705.

(2) Jones, P. A.; Baylin, S. B. The epigenomics of cancer. *Cell* **2007**, *128*, 683−692.

(3) Wilson, C. B.; Rowell, E.; Sekimata, M. Epigenetic control of T-helper-cell differentiation. *Nat. Rev. Immunol.* **2009**, *9*, 91−105.

(4) Tsankova, N.; Renthal, W.; Kumar, A.; Nestler, E. J. Epigenetic regulation in psychiatric disorders. *Nat. Rev. Neurosci.* **2007**, *8*, 355−367.

(5) Copeland, R. A.; Solomon, M. E.; Richon, V. M. Protein methyltransferases as a target class for drug discovery. *Nat. Rev. Drug Discovery* **2009**, *8*, 724−732.

(6) Cole, P. A. Chemical probes for histone-modifying enzymes. *Nat. Chem. Biol.* **2008**, *4*, 590−597.

(7) Falkenberg, K. J.; Johnstone, R. W. Histone deacetylases and their inhibitors in cancer, neurological diseases and immune disorders. *Nat. Rev. Drug Discovery* **2014**, *13*, 673−691.

(8) Milne, T. A.; Briggs, S. D.; Brock, H. W.; Martin, M. E.; Gibbs, D.; Allis, C. D.; Hess, J. L. MLL targets SET domain methyltransferase activity to Hox gene promoters. *Mol. Cell* **2002**, *10*, 1107−1117.

(9) Briggs, S. D.; Bryk, M.; Strahl, B. D.; Cheung, W. L.; Davie, J. K.; Dent, S. Y.; Winston, F.; Allis, C. D. Histone H3 lysine 4 methylation is mediated by Set1 and required for cell growth and rDNA silencing in Saccharomyces cerevisiae. *Genes Dev.* **2001**, *15*, 3286−3295.

(10) Milne, T. A.; Briggs, S. D.; Brock, H. W.; Martin, M. E.; Gibbs, D.; Allis, C. D.; Hess, J. L. MLL targets SET domain methyltransferase activity to Hox gene promoters. *Mol. Cell* **2002**, *10*, 1107−1117.

(11) Krivtsov, A. V.; Armstrong, S. A. MLL translocations, histone modifications and leukaemia stem-cell development. *Nat. Rev. Cancer* **2007**, *7*, 823−833.

(12) Nakamura, T.; Mori, T.; Tada, S.; Krajewski, W.; Rozovskaia, T.; Wassell, R.; Dubois, G.; Mazo, A.; Croce, C. M.; Canaani, E. ALL-1 is a histone methyltransferase that assembles a supercomplex of proteins involved in transcriptional regulation. *Mol. Cell* **2002**, *10*, 1119−1128.

(13) Shi, Y.; Lan, F.; Matson, C.; Mulligan, P.; Whetstine, J. R.; Cole, P. A.; Casero, R. A.; Shi, Y. Histone demethylation mediated by the nuclear amine oxidase homolog LSD1. *Cell* **2004**, *119*, 941−953.

(14) Kerenyi, M. A.; Shao, Z.; Hsu, Y. J.; Guo, G.; Luc, S.; O'Brien, K.; Fujiwara, Y.; Peng, C.; Nguyen, M.; Orkin, S. H. Histone demethylase Lsd1 represses hematopoietic stem and progenitor cell signatures during blood cell maturation. *eLife* **2013**, *2*, e00633.

(15) Metzger, E.; Wissmann, M.; Yin, N.; Müller, J. M.; Schneider, R.; Peters, A. H.; Günther, T.; Buettner, R.; Schüle, R. LSD1 demethylates repressive histone marks to promote androgen-receptor-dependent transcription. *Nature* **2005**, *437*, 436−439.

(16) Wang, J.; Hevi, S.; Kurash, J. K.; Lei, H.; Gay, F.; Bajko, J.; Su, H.; Sun, W.; Chang, H.; Xu, G.; Gaudet, F.; Li, E.; Chen, T. The lysine demethylase LSD1 (KDM1) is required for maintenance of global DNA methylation. *Nat. Genet.* **2009**, *41*, 125−129.

(17) Chen, C. S.; Sorensen, P. H.; Domer, P. H.; Reaman, G. H.; Korsmeyer, S. J.; Heerema, N. A.; Hammond, G. D.; Kersey, J. H. Molecular rearrangements on chromosome 11q23 predominate in infant acute lymphoblastic leukemia and are associated with specific biologic variables and poor outcome. *Blood* **1993**, *81*, 2386−2393.

(18) Mrozek, K.; Heinonen, K.; Lawrence, D.; Carroll, A. J.; Koduru, P. R.; Rao, K. W.; Strout, M. P.; Hutchison, R. E.; Moore, J. O.; Mayer, R. J.; Schiffer, C. A.; Bloomfield, C. D. Adult patients with de novo acute myeloid leukemia and t(9; 11)(p22; q23) have a superior outcome to patients with other translocations involving band 11q23: a cancer and leukemia group B study. *Blood* **1997**, *90*, 4532−4538.

(19) Hilden, J. M.; Dinndorf, P. A.; Meerbaum, S. O.; Sather, H.; Villaluna, D.; Heerema, N. A.; McGlennen, R.; Smith, F. O.; Woods, W. G.; Salzer, W. L.; Johnstone, H. S.; Dreyer, Z.; Reaman, G. H. Analysis of prognostic factors of acute lymphoblastic leukemia in infants: report on CCG 1953 from the Children's Oncology Group. *Blood* **2006**, *108*, 441−451.

(20) Okada, Y.; Feng, Q.; Lin, Y.; Jiang, Q.; Li, Y.; Coffield, V. M.; Su, L.; Xu, G.; Zhang, Y. hDOT1L links histone methylation to leukemogenesis. *Cell* **2005**, *121*, 167−178.

(21) Bitoun, E.; Oliver, P. L.; Davies, K. E. The mixed-lineage leukemia fusion partner AF4 stimulates RNA polymerase II transcriptional elongation and mediates coordinated chromatin remodeling. *Hum. Mol. Genet.* **2007**, *16*, 92−106.

(22) Krivtsov, A. V.; Feng, Z.; Lemieux, M. E.; Faber, J.; Vempati, S.; Sinha, A. U.; Xia, X.; Jesneck, J.; Bracken, A. P.; Silverman, L. B.; Kutok, J. L.; Kung, A. L.; Armstrong, S. A. H3K79 methylation profiles define murine and human MLL-AF4 leukemias. *Cancer Cell* **2008**, *14*, 355−368.

(23) For work from us, see the following: (a) Yao, Y.; Chen, P.; Diao, J.; Cheng, G.; Deng, L.; Anglin, J. L.; Prasad, B. V.; Song, Y. Selective inhibitors of histone methyltransferase DOT1L: design, synthesis, and crystallographic studies. *J. Am. Chem. Soc.* **2011**, *133*, 16746−16749. (b) Anglin, J. L.; Deng, L.; Yao, Y.; Cai, G.; Liu, Z.; Jiang, H.; Cheng, G.; Chen, P.; Dong, S.; Song, Y. Synthesis and structure-activity relationship investigation of adenosine-containing inhibitors of histone methyltransferase DOT1L. *J. Med. Chem.* **2012**, *55*, 8066−8074. (c) Deng, L.; Zhang, L.; Yao, Y.; Wang, C.; Redell, M. S.; Dong, S.; Song, Y. Synthesis, activity and metabolic stability of non-ribose containing inhibitors of histone methyltransferase DOT1L. *MedChemComm* **2013**, *4*, 822−826. (d) Liu, W.; Deng, L.; Song, Y.; Redell, M. DOT1L Inhibition Sensitizes MLL-Rearranged AML to Chemotherapy. *PLoS One* **2014**, *9*, e98270.

(24) For work from other groups, seethe following: (a) Daigle, S. R.; Olhava, E. J.; Therkelsen, C. A.; Majer, C. R.; Sneeringer, C. J.; Song, J.; Johnston, L. D.; Scott, M. P.; Smith, J. J.; Xiao, Y.; Jin, L.; Kuntz, K. W.; Chesworth, R.; Moyer, M. P.; Bernt, K. M.; Tseng, J. C.; Kung, A. L.; Armstrong, S. A.; Copeland, R. A.; Richon, V. M.; Pollock, R. M. Selective killing of mixed lineage leukemia cells by a potent small-molecule DOT1L inhibitor. *Cancer Cell* **2011**, *20*, 53−65. (b) Basavapathruni, A.; Jin, L.; Daigle, S. R.; Majer, C. R.; Therkelsen, C. A.; Wigle, T. J.; Kuntz, K. W.; Chesworth, R.; Pollock, R. M.; Scott, M. P.; Moyer, M. P.; Richon, V. M.; Copeland, R. A.; Olhava, E. J. Conformational adaptation drives potent, selective and durable inhibition of the human protein methyltransferase DOT1L. *Chem. Biol. Drug Des.* **2012**, *80*, 971−980. (c) Yu, W.; Chory, E. J.; Wernimont, A. K.; Tempel, W.; Scopton, A.; Federation, A.; Marineau, J. J.; Qi, J.; Barsyte-Lovejoy, D.; Yi, J.; Marcellus, R.; Iacob, R. E.; Engen, J. R.; Griffin, C.; Aman, A.; Wienholds, E.; Li, F.; Pineda, J.; Estiu, G.; Shatseva, T.; Hajian, T.; Al-Awar, R.; Dick, J. E.; Vedadi, M.; Brown, P. J.; Arrowsmith, C. H.; Bradner, J. E.; Schapira, M. Catalytic site remodelling of the DOT1L methyltransferase by selective inhibitors. *Nat. Commun.* **2012**, *3*, 1288. (d) Daigle, S. R.; Olhava, E. J.; Therkelsen, C. A.; Basavapathruni, A.; Jin, L.; Boriack-Sjodin, P. A.; Allain, C. J.; Klaus, C. R.; Raimondi, A.; Scott, M. P.; Waters, N. J.; Chesworth, R.; Moyer, M. P.; Copeland, R. A.; Richon, V. M.; Pollock, R. M. Potent inhibition of DOT1L as treatment for MLL-fusion leukemia. *Blood* **2013**, *122*, 1017−1025.

(25) Binda, C.; Valente, S.; Romanenghi, M.; Pilotto, S.; Cirilli, R.; Karytinos, A.; Ciossani, G.; Botrugno, O. A.; Forneris, F.; Tardugno, M.; Edmondson, D. E.; Minucci, S.; Mattevi, A.; Mai, A. Biochemical, structural, and biological evaluation of tranylcypromine derivatives as inhibitors of histone demethylases LSD1 and LSD2. *J. Am. Chem. Soc.* **2010**, *132*, 6827−6833.

(26) See recent reviews and the references therein. (a) Suzuki, T.; Miyata, N. Lysine demethylases inhibitors. *J. Med. Chem.* **2011**, *54*, 8236−8250. (b) Mould, D. P.; McGonagle, A. E.; Wiseman, D. H.; Williams, E. L.; Jordan, A. M. Reversible inhibitors of LSD1 as therapeutic agents in acute myeloid leukemia: clinical significance and progress to date. *Med. Res. Rev.* **2015**, *35*, 586−618.

(27) For more recent LSD1 inhibitors, see the following: (a) Neelamegam, R.; Ricq, E. L.; Malvaez, M.; Patnaik, D.; Norton, S.; Carlin, S. M.; Hill, I. T.; Wood, M. A.; Haggarty, S. J.; Hooker, J. M. Brain-penetrant LSD1 inhibitors can block memory consolidation. *ACS Chem. Neurosci.* **2012**, *3*, 120−128. (b) Zheng, Y. C.; Duan, Y. C.; Ma, J. L.; Xu, R. M.; Zi, X.; Lv, W. L.; Wang, M. M.; Ye, X. W.; Zhu, S.; Mobley, D.; Zhu, Y. Y.; Wang, J. W.; Li, J. F.; Wang, Z. R.; Zhao, W.; Liu, H. M. Triazole-dithiocarbamate based selective lysine specific demethylase 1 (LSD1) inactivators inhibit gastric cancer cell growth, invasion, and migration. *J. Med. Chem.* **2013**, *56*, 8543−8560. (c) Sorna, V.; Theisen, E. R.; Stephens, B.; Warner, S. L.; Bearss, D. J.; Vankayalapati, H.; Sharma, S. High-throughput virtual screening identifies novel N′-(1-phenylethylidene)-benzohydrazides as potent, specific, and reversible LSD1 inhibitors. *J. Med. Chem.* **2013**, *56*, 9496−9508. (d) Prusevich, P.; Kalin, J. H.; Ming, S. A.; Basso, M.;

Givens, J.; Li, X.; Hu, J.; Taylor, M. S.; Cieniewicz, A. M.; Hsiao, P. Y.; Huang, R.; Roberson, H.; Adejola, N.; Avery, L. B.; Casero, R. A., Jr.; Taverna, S. D.; Qian, J.; Tackett, A. J.; Ratan, R. R.; McDonald, O. G.; Feinberg, A. P.; Cole, P. A. A Selective Phenelzine Analogue Inhibitor of Histone Demethylase LSD1. *ACS Chem. Biol.* **2014**, *9*, 1284−1293. (e) Huang, Y.; Greene, E.; Stewart, T. M.; Goodwin, A. C.; Baylin, S. B.; Woster, P. M.; Casero, R. A. Inhibition of lysine-specific demethylase 1 by polyamine analogues results in reexpression of aberrantly silenced genes. *Proc. Natl. Acad. Sci. U. S. A.* **2007**, *104*, 8023−8028. (f) Huang, Y.; Stewart, T. M.; Wu, Y.; Baylin, S. B.; Marton, L. J.; Perkins, B.; Jones, R. J.; Woster, P. M.; Casero, R. A., Jr. Novel oligoamine analogues inhibit lysine-specific demethylase 1 and induce reexpression of epigenetically silenced genes. *Clin. Cancer Res.* **2009**, *15*, 7217−7228. (g) Sharma, S. K.; Wu, Y.; Steinbergs, N.; Crowley, M. L.; Hanson, A. S.; Casero, R. A., Jr.; Woster, P. M. (Bis)urea and (Bis)thiourea Inhibitors of Lysine-Specific Demethylase 1 as Epigenetic Modulators. *J. Med. Chem.* **2010**, *53*, 5197−5212. (h) Kutz, C. J.; Holshouser, S. L.; Marrow, E. A.; Woster, P. M. 3,5-Diamino-1,2,4-triazoles as a novel scaffold for potent, reversible LSD1 (KDM1A) inhibitors. *MedChemComm* **2014**, *5*, 1863−1870. (i) Hitchin, J. R.; Blagg, J.; Burke, R.; Burns, S.; Cockerill, M. J.; Fairweather, E. E.; Hutton, C.; Jordan, A. M.; McAndrew, C.; Mirza, A.; Mould, D.; Thomson, G. T.; Waddell, I.; Ogilvie, D. J. Development and evaluation of selective, reversible LSD1 inhibitors derived from fragments. *MedChemComm* **2013**, *4*, 1513−1522. (j) Culhane, J. C.; Wang, D.; Yen, P. M.; Cole, P. A. Comparative analysis of small molecules and histone substrate analogues as LSD1 lysine demethylase inhibitors. *J. Am. Chem. Soc.* **2010**, *132*, 3164−3176.

(28) Kahl, P.; Gullotti, L.; Heukamp, L. C.; Wolf, S.; Friedrichs, N.; Vorreuther, R.; Solleder, G.; Bastian, P. J.; Ellinger, J.; Metzger, E.; Schule, R.; Buettner, R. Androgen receptor coactivators lysine-specific histone demethylase 1 and four and a half LIM domain protein 2 predict risk of prostate cancer recurrence. *Cancer Res.* **2006**, *66*, 11341−11347.

(29) Schulte, J. H.; Lim, S.; Schramm, A.; Friedrichs, N.; Koster, J.; Versteeg, R.; Ora, I.; Pajtler, K.; Klein-Hitpass, L.; Kuhfittig-Kulle, S.; Metzger, E.; Schule, R.; Eggert, A.; Buettner, R.; Kirfel, J. Lysine-specific demethylase 1 is strongly expressed in poorly differentiated neuroblastoma: implications for therapy. *Cancer Res.* **2009**, *69*, 2065−2071.

(30) Lim, S.; Janzer, A.; Becker, A.; Zimmer, A.; Schule, R.; Buettner, R.; Kirfel, J. Lysine-specific demethylase 1 (LSD1) is highly expressed in ER-negative breast cancers and a biomarker predicting aggressive biology. *Carcinogenesis* **2010**, *31*, 512−520.

(31) Harris, W. J.; Huang, X.; Lynch, J. T.; Spencer, G. J.; Hitchin, J. R.; Li, Y.; Ciceri, F.; Blaser, J. G.; Greystoke, B. F.; Jordan, A. M.; Miller, C. J.; Ogilvie, D. J.; Somervaille, T. C. The histone demethylase KDM1A sustains the oncogenic potential of MLL-AF9 leukemia stem cells. *Cancer Cell* **2012**, *21*, 473−487.

(32) Dent, S. Y.; Chandra, J. The lasting influence of LSD1 in the blood. *eLife* **2013**, *2*, e00963.

(33) Lynch, J. T.; Harris, W. J.; Somervaille, T. C. LSD1 inhibition: a therapeutic strategy in cancer? *Expert Opin. Ther. Targets* **2012**, *16*, 1239−1249.

(34) Dhanak, D. Drugging the Cancer Epigenome. *Proceedings of the 104th Annual Meeting of the American Association for Cancer Research*, Washington, DC, April 6−10, 2013; AACR: Philadelphia, PA, 2013.

(35) Khan, M. N.; Suzuki, T.; Miyata, N. An overview of phenylcyclopropylamine derivatives: biochemical and biological significance and recent developments. *Med. Res. Rev.* **2013**, *33*, 873−910.

(36) Mimasu, S.; Umezawa, N.; Sato, S.; Higuchi, T.; Umehara, T.; Yokoyama, S. Structurally designed trans-2-phenylcyclopropylamine derivatives potently inhibit histone demethylase LSD1/KDM1. *Biochemistry* **2010**, *49*, 6494−6503.

(37) Tortorici, M.; Borrello, M. T.; Tardugno, M.; Chiarelli, L. R.; Pilotto, S.; Ciossani, G.; Vellore, N. A.; Bailey, S. G.; Cowan, J.; O'Connell, M.; Crabb, S. J.; Packham, G.; Mai, A.; Baron, R.; Ganesan, A.; Mattevi, A. Protein recognition by short peptide reversible inhibitors of the chromatin-modifying LSD1/CoREST lysine demethylase. *ACS Chem. Biol.* **2013**, *8*, 1677−1682.

(38) Stavropoulos, P.; Blobel, G.; Hoelz, A. Crystal structure and mechanism of human lysine-specific demethylase-1. *Nat. Struct. Mol. Biol.* **2006**, *13*, 626−632.

(39) Forneris, F.; Binda, C.; Adamo, A.; Battaglioli, E.; Mattevi, A. Structural basis of LSD1-CoREST selectivity in histone H3 recognition. *J. Biol. Chem.* **2007**, *282*, 20070−20074.

(40) *Schrödinger Suite*, version 2015; Schrödinger, LLC: New York, NY, 2015.

(41) Lin, H.; Yamashita, D. S.; Zeng, J.; Xie, R.; Wang, W.; Nidarmarthy, S.; Luengo, J. I.; Rhodes, N.; Knick, V. B.; Choudhry, A. E.; Lai, Z.; Minthorn, E. A.; Strum, S. L.; Wood, E. R.; Elkins, P. A.; Concha, N. O.; Heerding, D. A. 2,3,5-Trisubstituted pyridines as selective AKT inhibitors-Part I: Substitution at 2-position of the core pyridine for ROCK1 selectivity. *Bioorg. Med. Chem. Lett.* **2010**, *20*, 673−678.

(42) Lin, N.-H.; He, Y.; Holladay, M. W.; Ryther, K.; Li, Y. 3-Pyridyloxymethyl heterocyclic ether compounds useful in controlling chemical synaptic transmission. U.S. Patent 5,629,325, 1997.

(43) Ballell, L.; Bates, R. H.; Young, R. J.; Alvarez-Gomez, D.; Alvarez-Ruiz, E.; Barroso, V.; Blanco, D.; Crespo, B.; Escribano, J.; González, R.; Lozano, S.; Huss, S.; Santos-Villarejo, A.; Martín-Plaza, J. J.; Mendoza, A.; Rebollo-Lopez, M. J.; Remuiñan-Blanco, M.; Lavandera, J. L.; Pérez-Herran, E.; Gamo-Benito, F. J.; García-Bustos, J. F.; Barros, D.; Castro, J. P.; Cammack, N. Fueling open-source drug discovery: 177 small-molecule leads against tuberculosis. *ChemMedChem* **2013**, *8*, 313−321.

(44) Zheng, B.; Yao, Y.; Liu, Z.; Deng, L.; Anglin, J. L.; Jiang, H.; Prasad, B. V. V; Song, Y. Crystallographic Investigation and Selective Inhibition of Mutant Isocitrate Dehydrogenase. *ACS Med. Chem. Lett.* **2013**, *4*, 542−546.

(45) Deng, L.; Diao, J.; Chen, P.; Pujari, V.; Yao, Y.; Cheng, G.; Crick, D. C.; Prasad, B. V. V; Song, Y. Inhibition of 1-Deoxy-D-Xylulose-5-Phosphate Reductoisomerase by Lipophilic Phosphonates: SAR, QSAR and Crystallographic Studies. *J. Med. Chem.* **2011**, *54*, 4721−34.

(46) Deng, L.; Sundriyal, S.; Rubio, V.; Shi, Z.; Song, Y. Coordination Chemistry Based Approach to Lipophilic Inhibitors of 1-Deoxy-D-xylulose-5-phosphate Reductoisomerase. *J. Med. Chem.* **2009**, *52*, 6539−42.

(47) Zhang, L.; Deng, L.; Chen, F.; Yao, Y.; Wu, B.; Wei, L.; Mo, Q.; Song, Y. Inhibition of Histone H3K79 Methylation Selectively Inhibits Proliferation, Self-renewal and Metastatic Potential of Breast Cancer. *Oncotarget* **2014**, *5*, 10665−10677.

(48) Liu, Z.; Yao, Y.; Kogiso, M.; Zheng, B.; Deng, L.; Qiu, J. J.; Dong, S.; Lv, H.; Gallo, J. M.; Li, X.-N.; Song, Y. Inhibition of Cancer-Associated Mutant Isocitrate Dehydrogenases: Synthesis, SAR and Selective Antitumor Activity. *J. Med. Chem.* **2014**, *57*, 8307−8318.